JOURNAL OF VIROLOGY, July 2006, p. 6430–6440 Vol. 80, No. 13
0022-538X/06/$08.00+0 doi:10.1128/JVI.00044-06

Reverse Genetic Generation of Recombinant Zaire Ebola Viruses Containing Disrupted IRF-3 Inhibitory Domains Results in Attenuated Virus Growth In Vitro and Higher Levels of IRF-3 Activation without Inhibiting Viral Transcription or Replication

Amy L. Hartman, Jason E. Dover, Jonathan S. Towner, and Stuart T. Nichol*

Special Pathogens Branch, Division of Viral and Rickettsial Diseases, National Center for Infectious Diseases, Centers for Disease Control and Prevention, 1600 Clifton Rd., MS G-14, Atlanta, Georgia 30329

Received 6 January 2006/Accepted 18 April 2006

The VP35 protein of Zaire Ebola virus is an essential component of the viral RNA polymerase complex and also functions to antagonize the cellular type I interferon (IFN) response by blocking activation of the transcription factor IRF-3. We previously mapped the IRF-3 inhibitory domain within the C terminus of VP35. In the present study, we show that mutations that disrupt the IRF-3 inhibitory function of VP35 do not disrupt viral transcription/replication, suggesting that the two functions of VP35 are separable. Second, using reverse genetics, we successfully recovered recombinant Ebola viruses containing mutations within the IRF-3 inhibitory domain. Importantly, we show that the recombinant viruses were attenuated for growth in cell culture and that they activated IRF-3 and IRF-3-inducible gene expression at levels higher than that for Ebola virus containing wild-type VP35. In the context of Ebola virus pathogenesis, VP35 may function to limit early IFN-β production and other antiviral signals generated from cells at the primary site of infection, thereby slowing down the host's ability to curb virus replication and induce adaptive immunity.

The recent outbreak of Marburg hemorrhagic fever in Angola, West Africa, involved at least 252 infections and 227 deaths, resulting in a case fatality rate of approximately 90% (Republic of Angola Ministry of Health, direct communication). This serves as a reminder that members of the family *Filoviridae*, which include both Marburg and Ebola viruses, cause some of the most severe viral hemorrhagic fevers known. While human infections by these viruses generally occur sporadically, they can have a large public health and economic impact on the affected region.

On the basis of data obtained from previous outbreaks, human infections with the Zaire strain of Ebola virus frequently cause a rapidly fatal disease termed Ebola hemorrhagic fever (EHF) that results in death 7 to 11 days after the onset of symptoms (25, 40). Hallmarks of EHF in humans and nonhuman primates include vascular and coagulation defects, which frequently lead to bruising, bleeding, blood in urine/feces, and disseminated intravascular coagulation (DIC) (11, 18). Viremia increases dramatically in infected patients and can reach levels near 1×10^9 viral RNA copies/ml of serum 3 days after the onset of symptoms in fatal cases (40). Immunosuppression is a hallmark of fatal EHF cases, where little or no virus-specific immunoglobulin G (IgG) and IgM antibody responses can be found (1, 26, 27, 40). Conversely, nonfatal cases have 2 to 3 log units less virus in the blood, and these patients develop detectable IgG antibody responses (40).

Ebola virus initially replicates within macrophages and dendritic cells (DCs) at the primary site of infection, and it is then transported to regional lymph nodes where it gains access to a large pool of susceptible cells (17, 20, 38). There is some evidence that early infection of macrophages and dendritic cells may impair their ability to induce adaptive immunity and thus could potentially contribute to the immunosuppression seen in fatal EHF cases (8, 10, 22, 30). Macrophages and dendritic cells infected with Ebola virus are able to initiate coagulation and secrete inflammatory cytokines but are unable to stop the spread of the virus systemically, most likely by their inability to provide costimulatory help to T cells (10). In addition, Ebola virus-infected macrophages express tissue factor on the cell surface, which triggers DIC (18). Indeed, many of the characteristics of EHF, including DIC, bystander lymphocyte apoptosis, and dysregulated inflammatory cytokine production are all similar to those seen in septic shock induced by bacterial infections (12).

The type I interferon (IFN) system is a critical component of the first line of defense against invading viruses, and it also plays a role in the subsequent induction of adaptive immunity. Within a short period of time after viral infection, several transcription factors are quickly activated, including interferon regulatory factor 3 (IRF-3), NF-κB, and ATF-2/c-JUN, which in turn induce the expression of beta IFN (IFN-β) and other antiviral genes (reviewed in reference 21). One of the critical transcription factors, IRF-3, is constitutively present in the cytoplasm and becomes activated by phosphorylation at serine/threonine residues in the carboxy terminus. Phosphorylation

* Corresponding author. Mailing address: Special Pathogens Branch, Division of Viral and Rickettsial Diseases, National Center for Infectious Diseases, Centers for Disease Control and Prevention, 1600 Clifton Rd., MS G-14, Atlanta, GA 30329. Phone: (404) 639-1115. Fax: (404) 639-1118. E-mail: stn1@cdc.gov.

then leads to dimerization and nuclear translocation, where the active form of IRF-3 interacts with CBP and p300 to induce the expression of IFN-β and other immediate-early antiviral genes, such as RANTES, ISG56, ISG54, ISG15, inducible nitric oxide synthase, and interleukin 15 (21). Some of these genes curb viral replication at the cellular level, others act in a paracrine manner to induce an antiviral state in neighboring cells, while others, such as inflammatory cytokines, signal to the immune system that an invasion by a pathogen has occurred. With respect to induction of adaptive immunity, alpha/beta interferon (IFN-α/β) secreted by an infected macrophage or DC can act as an adjuvant by inducing the maturation of uninfected macrophages and DCs, thus enhancing their ability to prime naïve T cells and induce antibody responses (28). Because of the potency of the type I IFN system, many viruses have developed ways to avoid or antagonize one or more of its components. Blocking the production and/or action of IFN-α/β could prevent direct antiviral effects, dysregulate the cytokine/chemokine cascade, and/or delay the timely induction of adaptive antibody responses.

One probable cause for the profound immunosuppression seen in EHF patients may be inhibition of IRF-3 activation by the Ebola virus VP35 protein (3, 4, 23). Basler et al. have shown that the Ebola virus VP35 protein inhibits the activation of IRF-3 in vitro and that infection with Ebola virus does not induce IRF-3 activation (3). The role that VP35-mediated IRF-3 inhibition plays in viral replication and disease pathogenesis remains to be determined. However, VP35 of Ebola virus has another role during virus infection. Similar to the phosphoproteins (P proteins) of paramyxoviruses, VP35 is an essential cofactor in the ribonucleoprotein (RNP) complex, which consists of the NP, VP30, VP35, and L proteins (35). The RNP complex proteins tightly associate with the RNA genome and catalyze viral transcription and replication.

We previously identified an IRF-3 inhibitory motif within the C terminus of the Ebola virus VP35 protein (23). This motif shows similarities with the RNA-binding domain of the influenza A virus NS1 protein, which is a well-characterized viral IFN antagonist. We also identified several basic amino acids within the C-terminal motif of VP35 that are critical for the ability to block IRF-3 activation in transfected cells in vitro. In the present study, we continue the investigation into IFN antagonism mediated by VP35 and demonstrate two significant findings. First, mutations that inactivate the IRF-3 inhibitory domain do not significantly inhibit the viral transcription/replication function of the protein, and thus, the two functions of the protein are separable. Second, we used reverse genetics to recover recombinant Ebola virus containing mutations in the IRF-3 inhibitory domain of VP35. The recombinant viruses were unable to block IRF-3 activation as effectively as the wild-type (wt) virus, and as a result, activated IRF-3 and the IRF-3-inducible gene RANTES at higher levels. The recombinant viruses were also severely attenuated for growth in several cell lines compared to virus with an intact IRF-3 inhibitory domain. This study represents an important step in elucidating the role of VP35 in the pathogenesis of EHF.

MATERIALS AND METHODS

Cells and viruses. Vero E6 and 293T cells were maintained in Dulbecco's modified Eagle's medium (DMEM) containing 100 U/ml penicillin, 100 U/ml streptomycin, and 10 mM HEPES buffer (complete) supplemented with 10% fetal bovine serum (FBS) unless otherwise indicated. Huh7 hepatocytes (obtained from Apath, LLC) were cultured in complete DMEM as described above and further supplemented with nonessential amino acids and 10% FBS. The U937 human monocyte cell line (ATCC CRL-1593.2) was cultured in complete RPMI medium containing 10% FBS. Ebola virus infections were performed in complete DMEM containing 2% FBS. All work with infectious Ebola virus was performed within positive-pressure suits in the biosafety level 4 laboratory at the Centers for Disease Control and Prevention. When necessary, the infectivity of samples was inactivated with 2×10^6 to 5×10^6 rads of cobalt 60 radiation from a Gammacell irradiator.

Immunofluorescence. For transfection-based assays, Vero E6 cells were seeded into 24-well plates containing coverslips at a concentration of 2.5×10^4 cells/well. The following day, the cells were transfected using TransIT-LT1 transfection reagent (Mirus Bio). Each well received 150 ng of a hemagglutinin (HA)-tagged IRF-3 plasmid and 150 ng of one of the pcDNA-VP35 plasmids along with 0.9 μl of TransIT-LT1 in 50 μl Optimem. Twenty-four hours after transfection, the cells were infected with the Cantell strain of Sendai virus (SeV) (ATCC VR-907) at a multiplicity of infection (MOI) of 1 for 1 h at room temperature. After infection, the cells were cultured in complete DMEM containing 2% FBS for 6 h. At 6 h postinfection (h.p.i.), the cells on the coverslips were fixed with 10% neutral buffered formalin for 30 min, washed three times with phosphate-buffered saline (PBS) containing 1% bovine serum albumin, and then permeabilized with PBS containing 0.1% Triton X-100 for 3 min. After the cells on the coverslips were washed, they were stained with an anti-HA-Alexafluor-488 (1:1,000; Molecular Probes), a rabbit polyclonal anti-Ebola virus (1:500), followed by secondary staining with a goat anti-rabbit Alexafluor-594 (1:500; Molecular Probes). The cells were then mounted using ProLong Gold antifade reagent with 4′,6′-diamidino-2-phenylindole (DAPI) (Molecular Probes). To determine the percentage of cells containing nuclear IRF-3, we counted six random panels from each well (250 to 500 cells total), and the percentage of cells with nuclear versus cytoplasmic IRF-3 was calculated.

For analysis of IRF-3 localization using live recombinant Ebola virus (recEbo), Vero cells were plated on coverslips as described above. The following day, the cells were infected with the indicated Ebola viruses at an MOI of 2. The virus was adsorbed for 1 h at 37°C, after which the inoculum was removed and replaced with 500 μl of complete DMEM containing 2% FBS. Immediately following adsorption, the cells were transfected with 300 ng of an HA-tagged IRF-3 plasmid using TransIT-LT1 reagent. Twenty-four hours postinfection, the cells were fixed and stained with the antibodies indicated above. For quantification, approximately 100 to 200 cells were counted per coverslip, and the ratio of nuclear versus cytoplasmic IRF-3 was calculated.

CAT minigenome transcription/replication assay. The negative-sense 3E-5E chloramphenicol acetyltransferase (CAT) minigenome has been described previously (35). 293T cells were seeded into six-well plates so that they would be 60% confluent by the following day. Prior to transfection, the medium was removed from each well, and 1 ml of complete DMEM containing 2% FBS was added. For each well, the following plasmids and amounts were used: 3E-5E minigenome, 1 μg; pT7-pol, 1 μg; pCEZ-NP, 1 μg; pCEZ-VP35, 0.5 μg; pCEZ-VP30, 0.3 μg; and pCEZ-L, 1 μg. For each well, 10 μl of TransIT-293 transfection reagent (Mirus Bio) was diluted in 200 μl Optimem. The plasmids were combined together and added to the TransIT/Optimem mixture. After 30 min, the TransIT-DNA mixture was added to each well, and the plates were incubated overnight at 37°C. The following day, the medium was removed from each well and replaced with 2 ml complete DMEM containing 2% FBS. Forty-eight hours afterwards, the cells were lysed in buffer containing complete mini protease inhibitor cocktail set II (Roche), and CAT levels were measured using an enzyme-linked immunosorbent assay (ELISA) according to the manufacturer's instructions (Roche). All transfections were performed in duplicate, and each sample was run in duplicate in the CAT ELISA. The sensitivity of the CAT ELISA is 50 pg/ml. Results shown are representative of three different experiments.

Western blots. Cell lysates from transfections were subjected to sodium dodecyl sulfate-polyacrylamide gel electrophoresis (SDS-PAGE) using the NuPage bis-tris system (Invitrogen). Samples were loaded onto 10% bis-tris gels and electrophoresed for 50 min at 200 V. Proteins were transferred to nitrocellulose membranes using the X-Cell II blot module (Invitrogen) and then probed with an anti-VP35 monoclonal antibody (1:2,000) or an antiactin control (1:1,000) (Chemicon). Blots were developed using the Western Breeze chemiluminescence detection system (Invitrogen) and exposed to film. Protein expression levels were determined using the AlphaImager EC camera and densitometry software.

TABLE 1. Characteristics of VP35 proteins containing alanine substitutions

VP35 construct	Inhibition of ISG56 expression[a,b]	Inhibition of IFN-β production[a,b]	Inhibition of IRF-3 activation[b]	Support of minigenome[c]	Rescue of Ebola virus[c]	Virus growth in culture[d]	Induction of RANTES[e]
wt VP35	+	+	+	+	+	+++	+
R305A	+	+/−	+/−	+	+	++	++
K309A	+/−	+/−	+/−	+	+	N/A	N/A
R312A	−	−	−	+	+	+	+++
R305AA K309A	−	−	−	+	+	N/A	N/A
K309 R312A	−	−	−	+	+	N/A	N/A
R300Term	−	−	N/A[f]	N/A	N/A	N/A	N/A

[a] Data from Hartman et al. (23).
[b] Symbols: +, inhibition; +/−, weak inhibition; −, no inhibition.
[c] Symbol: +, positive.
[d] Symbols: +, growth; ++, moderate level of growth; +++, high level of growth.
[e] Symbols: +, induction; ++, moderate level of induction; +++, high level of induction.
[f] N/A, not applicable.

Rescue of Ebola virus containing mutations in VP35. Generation of the parental full-length infectious clone of the Ebola virus genome has been described previously (39). Specific mutations were introduced into the VP35 gene using the overlapping PCR method. Each clone was sequenced entirely to ensure no additional unintentional mutations were introduced. The virus was rescued using the minigenome method described above except that cocultures of a 50:50 mixture of Vero E6 cells and 293T cells were used. For each full-length clone, 1 μg was used per well for the transfection, along with the indicated amounts of support plasmids given above. Each rescue was performed in duplicate. Approximately 4 days after transfection, the supernatant from each well was transferred to a T25 flask of Vero E6 cells, and the flasks were cultured 7 to 14 days longer, with the medium changed by 7 days. Cytopathic effect (CPE) was evident by 7 to 10 days posttransfer. When extensive CPE was noted, the flasks were frozen at −80°C. Following thawing, the supernatants from these flasks were clarified by centrifugation and used to infect roller bottles of Vero E6 cells for generation of passage 1 (P1) stocks. By 3 to 5 days postinfection, CPE was extensive and the bottles were frozen at −80°C. The titer of each stock was determined by standard immunoplaque assay (40). During all virus infections described above, cells were cultured in complete DMEM containing 2% FBS. The VP35 gene from each P1 virus stock was sequenced to confirm that the intended mutation(s) was present. In addition, each virus was passed 10 times on Vero E6 cells, and the VP35 gene was again sequenced to confirm the mutations. No reversions or compensatory mutations were found.

Growth of recombinant Ebola viruses in various cell lines. Growth curves of VP35 mutant viruses were generated by infecting Vero E6 cells at an MOI of either 2 or 0.02. One day prior to infection, 4×10^5 cells were plated per well of a 24-well plate. The following day, the cells were infected with the indicated viruses in a total volume of 250 μl medium per well. The virus was adsorbed for 2 h at 37°C, after which the inocula were removed. Each well was washed three times with PBS and then cultured in 1 ml complete DMEM containing 2% FBS. At each time point postinfection, the supernatants were harvested and the amount of infectious virus present was determined by immunoplaque assay (40). The amount of RANTES protein in each supernatant sample was determined by a RANTES ELISA kit (Biosource) according to the manufacturer's instructions. For growth curves involving U937 macrophages, 1×10^6 monocytes were seeded per well of a 24-well plate in the presence of 100 ng/ml phorbol 12-myristate 13-acetate (PMA; Sigma). Twenty-four hours later, the cells had attached and the PMA was removed and replaced with fresh RPMI medium for another 48 h. The cells were then infected as described above. For growth curves involving HuH7 cells, 1×10^5 cells were seeded per well 2 days prior to infection as described above.

RESULTS

Disruption of the IRF-3 inhibitory domain of Ebola virus VP35 restores SeV-induced activation of IRF-3. In transfection-based assays, the wild-type VP35 protein from Zaire Ebola virus prevented activation of the IRF-3-responsive promoter ISG56 by SeV infection, and this block was due to an inhibition of IRF-3 activation (3, 4, 23, 24). Our previous work has shown that alanine substitutions in an IRF-3 inhibitory motif within the C terminus of VP35 render the protein unable to prevent activation of ISG56, indicating the IRF-3 inhibitory domain has been disrupted (summarized in Table 1) (23). Within the IRF-3 inhibitory domain, the R312A single mutation, as well as the R305A K309A and K309A R312A double mutations, restored high levels of both ISG56 activation and IFN-β protein production after SeV infection compared to those induced by wt VP35.

To further characterize the effects of the VP35 mutations directly on IRF-3 activation, we examined IRF-3 localization by immunofluorescence (Fig. 1). Vero E6 cells were transfected with plasmids encoding HA-tagged IRF-3 and/or one of the VP35 plasmids. Twenty-four hours after transfection, the cells were infected with SeV for 6 h and then fixed and stained using anti-HA (green) and anti-Ebola virus (red) antibodies.

In cells transfected with an empty-vector control plasmid without SeV infection, IRF-3 localized exclusively in the cytoplasm, which is indicative of an inactive state (Fig. 1A, top row). SeV infection resulted in the majority of cells containing IRF-3 in the nucleus, a sign of activation (Fig. 1A, second row). When the wild-type VP35 plasmid was cotransfected under the above conditions, IRF-3 was retained exclusively in the cytoplasm after SeV infection, as evidenced by the "pothole" staining of cells (Fig. 1A, third row). However, when the panel of VP35 mutant proteins was coexpressed with IRF-3, various degrees of IRF-3 activation and nuclear accumulation were seen (Fig. 1B), which corresponded to our previous results with the ISG56 reporter gene (23). For the R305A and K309A single mutations, there were relatively few cells with nuclear IRF-3; however, several could be identified, and there were more than seen in the wt VP35 well. For the R312A, R305A K309A, and K309A R312A mutants, substantially more activated nuclear IRF-3 was observed, and the IRF-3 expression correlated with mutant VP35 expression for the majority of cells (Fig. 1A, bottom row). For quantitative purposes, the number of cells containing nuclear IRF-3 was determined by counting six random panels from each coverslip, and the data were normalized to the empty-vector control well (Fig. 1B). This experiment was repeated twice using 150 ng/well of the VP35 plasmids, and similar results were obtained using various doses of either 50 ng/well or 300 ng/well of the VP35 plasmids.

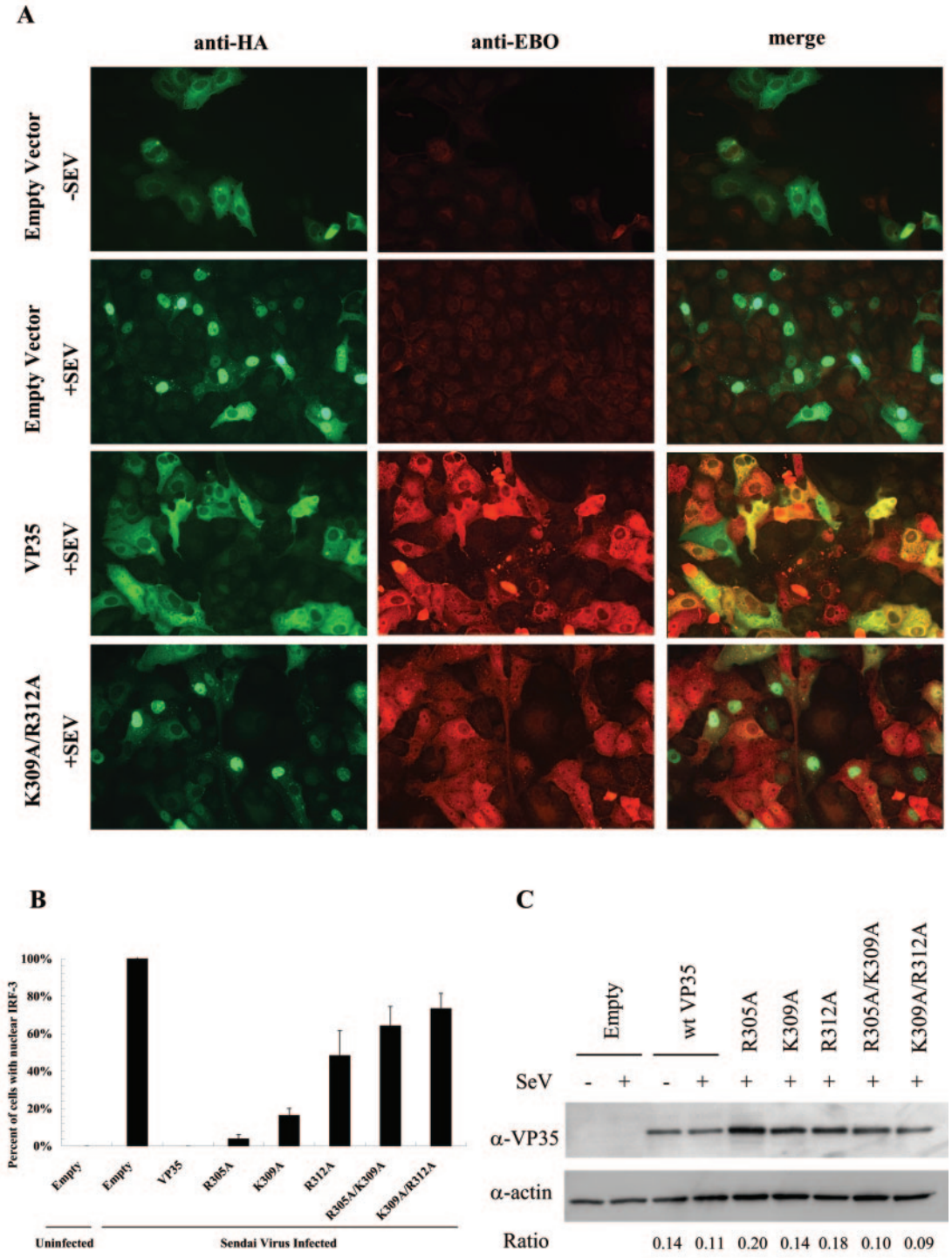

FIG. 1. Effects of mutations in the C-terminal domain of VP35 on IRF-3 activation. A) Localization of IRF-3. Vero E6 cells were transfected with HA-tagged IRF-3 and VP35 expression plasmids. Twenty-four hours later, the cells were infected with Sendai virus (+SEV). Six hours postinfection, the cells were fixed and stained with anti-HA (green) or polyclonal anti-Ebola virus (anti-EBO) (red) antibodies. A merged image is shown in the far right panels. Cells transfected with an empty vector (top two rows) show background levels of anti-Ebola virus staining which is distinguishable from wells transfected with VP35 plasmids. B) Percentage of cells with nuclear IRF-3 shown in a graph. For each coverslip, six random fields were chosen and the percentage of cells with nuclear versus cytoplasmic IRF-3 was determined. In total, approximately 250 to 500 cells were counted per sample. The results were averaged, and the standard deviation (error bar) is shown. These data are representative of four independent experiments using various amounts of the VP35 plasmids. C) Lysates made from parallel transfections were subjected to SDS-PAGE and Western blotting for VP35 and actin (loading control). Expression levels of each VP35 protein were measured using a densitometer and normalized to actin expression, which is expressed as a ratio below the panel. α-VP35, anti-VP35 antibody; α-actin, α-actin antibody.

The results are very similar to our previous data with the ISG56 reporter plasmid and IFN-β secretion (Table 1), confirming that both the reporter plasmid and cytokine production are suitable indicators of IRF-3 activation (23).

To ensure that the differences in IRF-3 activation seen here were not due to differences in the expression level of VP35 from the transfected plasmids, we performed SDS-PAGE and Western blotting on parallel lysates from the above transfections (Fig. 1C). Blots were probed with anti-VP35 or anti-actin (as a loading control), and the ratio of VP35 to actin expression is indicated below each lane. Expression levels were similar for all samples, and the expression level did not correlate with the amount of IRF-3 activation. These data suggest that the specific mutations shown here within the IRF-3 inhibitory domain result in VP35 proteins that are unable to fully prevent the activation of IRF-3.

The viral transcription/replication and IRF-3 inhibitory functions of VP35 are separable. Since VP35 is an essential cofactor in viral transcription and replication as part of the RNP complex, we determined whether the IRF-3 inhibitory domain mutations disrupt the ability of VP35 to function in viral transcription/replication. To do this, we used an Ebola virus minigenome system which has been used to extensively study the transcription/replication properties of Ebola virus (35). This system provides a reliable and proven method for examining viral transcription/replication without the confounding effects of IFN antagonism that would be present during a live virus infection. The minireplicon contains the chloramphenicol acetyltransferase gene in the negative sense flanked by authentic Ebola virus leader and trailer sequences. Transfection of this plasmid, along with specific ratios of plasmids containing the four nucleocapsid proteins (NP, VP35, VP30, and L) will result in a functional RNP complex, and transcription/replication will take place, leading to expression of the CAT gene. For these experiments, support plasmids containing either the wild-type VP35 sequence or one of the VP35 mutants were tested. If one of the mutations in VP35 renders it nonfunctional for transcription/replication, no CAT activity will be detected. The amount of VP35 plasmid used for each transfection was 0.5 μg, which has previously been determined to be the lowest optimal amount that will promote rescue of the minigenome (35).

The five VP35 proteins containing alanine substitutions in the IRF-3 inhibitory domain induced CAT expression levels that were similar to those induced by the wild-type VP35 protein (Fig. 2), whereas eliminating the L-polymerase plasmid resulted in zero CAT activity (negative control). While there was some variation within the mutants tested, repeated experiments showed that all five VP35 mutants could consistently promote substantial transcription/replication of the minireplicon. Western blots revealed that expression of VP35 from the panel of plasmids was similar and did not correlate with the amount of transcription/replication seen. These data suggest that the two functions of VP35, transcription/replication and the inhibition of IRF-3 activation, are separable.

Infectious recombinant Ebola viruses containing mutations within the IRF-3 inhibitory domain of VP35 are attenuated for growth in Vero E6 cells. To gain insight into the importance of VP35-mediated IRF-3 inhibition on virus growth, we used reverse genetics to generate infectious recombinant Ebola virus

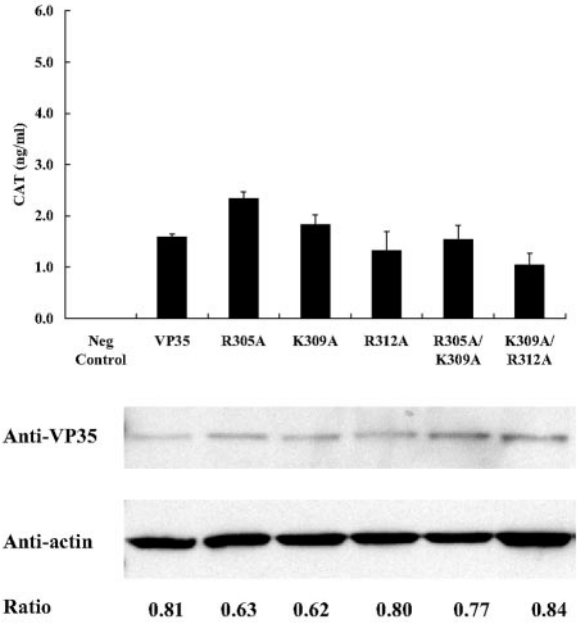

FIG. 2. Effects of mutations in the IRF-3 inhibitory domain of VP35 on viral transcription/replication. The 3E-5E CAT minigenome transcription/replication system was used to determine the effects of VP35 mutations on viral transcription. 293T cells were transfected in six-well plates with the 3E-5E minigenome (1 μg) along with expression plasmids for pT7-pol (1 μg), pCEZ-NP (1 μg), pCEZ-VP35 (0.5 μg), pCEZ-VP30 (0.3 μg), and pCEZ-L (1 μg). Forty-eight hours posttransfection, the cells were lysed, and CAT levels were measured by an ELISA. Results shown are averages of wells transfected in duplicate and are representative of three independent experiments. Lysates were subjected to SDS-PAGE and Western blotting to determine VP35 and actin expression levels, and expression ratios were calculated as described in the legend to Fig. 1. Neg Control, negative control.

encoding the IRF-3 inhibitory domain mutations within VP35. Generation of the parental infectious full-length clone of the Ebola virus genome has been described previously (39). Specific mutations were introduced into the VP35 gene of the full-length clone using the overlapping PCR method. The full-length clones were transfected into a mixture of VeroE6 and 293T cells along with the support expression plasmids for NP, L, VP30, and VP35. Recombinant virus was successfully rescued from clones containing each of the five VP35 mutations (Table 1), thus confirming that none of the mutations significantly hamper virus transcription or replication. In addition, there were no apparent differences in plaque size compared to the wild-type virus, and high-titer stocks were generated with each virus.

The ability of the recEBO-VP35/R305A and recEBO-VP35/R312A recombinant viruses to replicate in Vero E6 cells was assessed using both low and high multiplicities of infection (Fig. 3A and B, respectively). After the cells were seeded, Vero E6 cells were infected with each virus at an MOI of 2 or 0.02, and virus production was measured in the supernatants over time by a standard immunoplaque assay (40). At a low MOI, growth of the recEBO-VP35/R312A virus was 100-fold less than the recombinant Ebola virus containing the authentic VP35 sequence (recEBO-VP35/WT) at all time points exam-

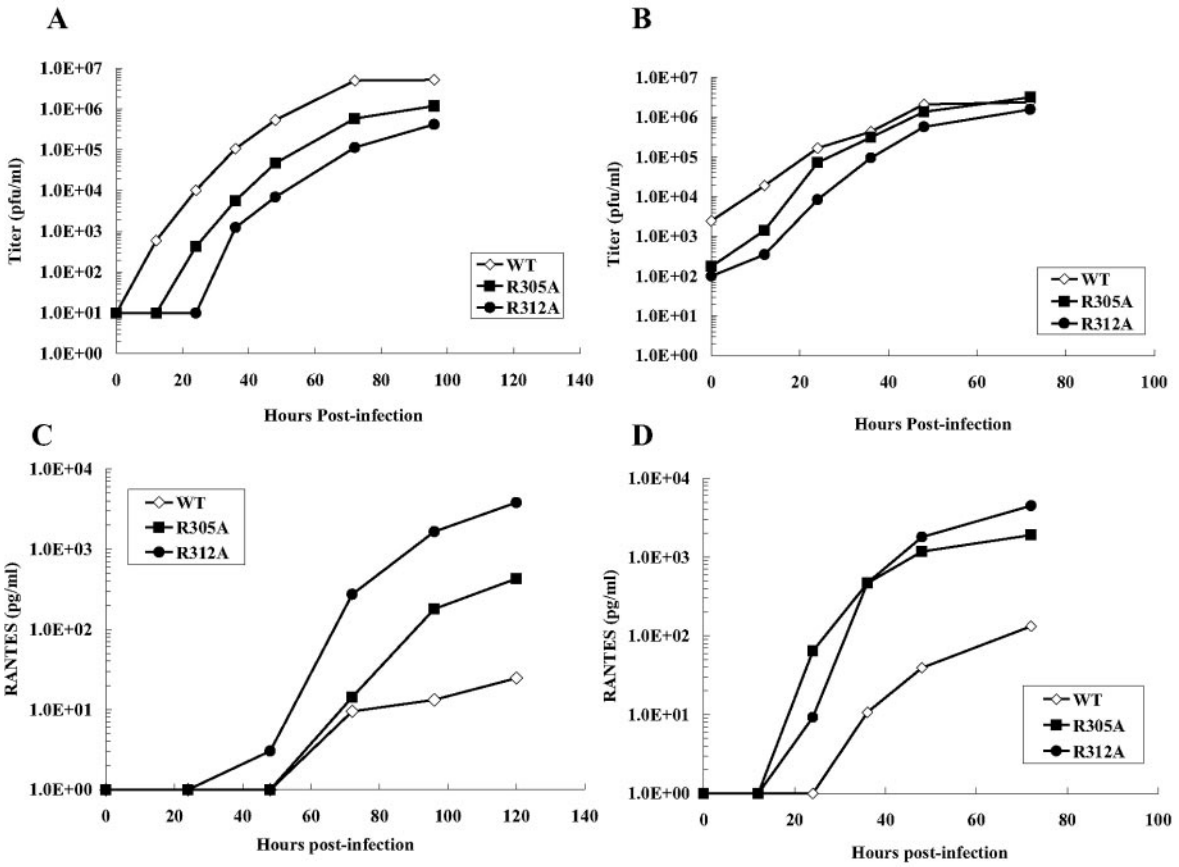

FIG. 3. Growth of recombinant Ebola viruses and production of RANTES during infection of Vero E6 cells with recombinant Ebola viruses. The growth of the recEBO-VP35/wt, recEBO-VP35/R305A, and recEBO-VP35/R312A viruses was measured in Vero E6 cells at an MOI of 0.02 (A) or 2 (B). Virus titer was determined by standard immunoplaque assay. RANTES was measured in the supernatants from the growth curves by an ELISA. The cells had been infected at an MOI of 0.02 (C) or 2 (D).

ined (Fig. 3A). Surprisingly, the recEBO-VP35/R305A virus was decreased in growth by 10-fold compared to the wt virus. While infectious virus was recovered from wells infected with the recEBO-VP35/WT virus as early as 12 h.p.i., none was detected in the recEBO-VP35/R305A and recEBO-VP35/R312A virus-infected wells until 24 and 36 h.p.i., respectively. These data suggest that emergence of virus and overall virus production are delayed and significantly diminished compared to the recEBO-VP35/WT virus. At a high-MOI infection, similar results were obtained, but the differences were less dramatic (Fig. 3B). The recEBO-VP35/R305A and recEBO-VP35/R312A viruses were attenuated especially at the early time points postinfection. These data suggest that the two recombinant Ebola viruses examined here that contain mutations in the IRF-3 inhibitory domain of VP35 display a measurable defect in growth in Vero E6 cells. Since the minigenome results showed that all five mutant VP35 proteins could function in viral transcription/replication as well as wt VP35, differences in growth of the recombinant viruses in cell culture are most likely due to alterations in the IRF-3 inhibitory capacity of the proteins.

Recombinant Ebola viruses with mutations in the IRF-3 inhibitory domain of VP35 induce higher levels of RANTES production in Vero E6 cells. To determine whether the differences in virus growth seen in Fig. 3A and B were due to a differential ability to activate IRF-3 after virus infection, we measured the amount of an IRF-3-inducible protein in the supernatant of the virus growth curves. Because Vero E6 cells have an inherent defect in the synthesis of IFN-β (33), we used the chemokine RANTES as a marker for early IRF-3 gene induction. IRF-3 has been documented to directly initiate the early transcription of a number of genes, one of which is IFN-β, but others include RANTES, interleukin 15, inducible nitric oxide synthase, ISG15, ISG54, and ISG56 (reviewed in reference 21). The purpose of measuring RANTES production here, therefore, is to have a read-out for early IRF-3 activation, and the RANTES gene serves this purpose as well as IFN-β. The RANTES promoter has been shown to be directly activated by cooperation between IRF-3 and NF-κB (19), and binding of IRF-3 to ISRE elements in the RANTES promoter is required for early expression (29). Therefore, RANTES expression is IRF-3 dependent. An ELISA performed on the supernatants from the growth curves showed a striking inverse correlation between virus production (Fig. 3A and B) and RANTES secretion (Fig. 3C and D). After a low MOI, cells infected with the recEBO-VP35/R312A virus secreted 100-fold more RANTES into the supernatant (Fig. 3C) while producing 100-fold-less infectious virus than the recEBO-VP35/WT virus

(Fig. 3A). RANTES secretion by cells infected with the recEBO-VP35/R305A virus was intermediate in comparison to the other two viruses, being approximately 10-fold higher than the recEBO-VP35/WT virus. At a high MOI, the results were similar (Fig. 3D). The recEBO-VP35/WT virus secreted the least amount of RANTES (by 100-fold) compared to the two viruses with mutations in the IRF-3 inhibitory domain of VP35. Because we found no differences in the abilities of the mutant VP35 proteins to promote viral transcription/replication, these results imply that the attenuated virus growth may be due to the inability to block IRF-3 activation as effectively as the virus containing the authentic VP35 protein.

The recEbo-VP35/R312A virus is attenuated for growth in both macrophage and hepatocyte cell lines. To determine whether the findings in Vero cells can be extended to cells that are able to synthesize IFN-β, we examined the ability of the recEbo-VP35/R312A virus to grow in two other cell lines: U937 macrophages and Huh7 hepatocytes. Both cell lines are physiologically relevant for the study of Ebola virus infections because they represent important target cells for virus infection. There is increasing evidence that, in controlled studies in rodents and nonhuman primates, macrophages are the initial target cells of Ebola virus at the primary site of infection (17, 20, 38) and thus may play a crucial role in the early events leading to virus dissemination. In addition, the liver is also a major target of virus infection during the later stages of disease, and fatal cases of both human and animal models of Ebola virus infection generally have severe virus-induced necrosis in the liver (9, 14, 20, 38, 43).

U937 monocytes were treated with PMA for 3 days to induce differentiation into macrophages and then infected with either the recEbo-VP35/WT or recEbo-VP35/R312A virus at an MOI of 0.02. Plaque assays for virus titer at each time point revealed substantial virus growth in cells infected with the recEbo-VP35/WT virus, but strikingly little virus growth was seen in cells infected with recEbo-VP35/R312A virus (Fig. 4A). In addition, higher levels of RANTES and IFN-β secretion were seen from cells infected with the recEbo-VP35/R312A virus compared to cells infected with recEbo-VP35/WT (data not shown).

Subsequently, Huh7 cells were seeded and infected with the above viruses at an MOI of 0.02 as well. The recEbo-VP35/R312A virus was severely decreased in growth (by 100-fold) compared to the recEbo-VP35/WT virus at all time points tested (Fig. 4B). Similarly to the results with Vero cells, the recEbo-VP35/R312A virus was attenuated by 100-fold at all time points examined in both macrophages as well as hepatocyte cell lines. Therefore, the severe growth defect that the recEbo-VP35/R312A virus has in Vero cells is comparable to results found in physiologically relevant cell lines like U937 and Huh7.

Recombinant Ebola viruses with mutations in the IRF-3 inhibitory domain of VP35 have a reduced ability to inhibit IRF-3 activation compared to the wild-type Ebola virus. To determine whether the differences in Ebola virus growth and RANTES secretion seen in Fig. 3 and 4 are due to a differential ability to activate IRF-3 after virus infection, we used immunofluorescence to examine the localization of IRF-3 during infection with the recombinant Ebola viruses. Vero E6 cells were infected with recEBO-VP35/WT virus or one of the VP35

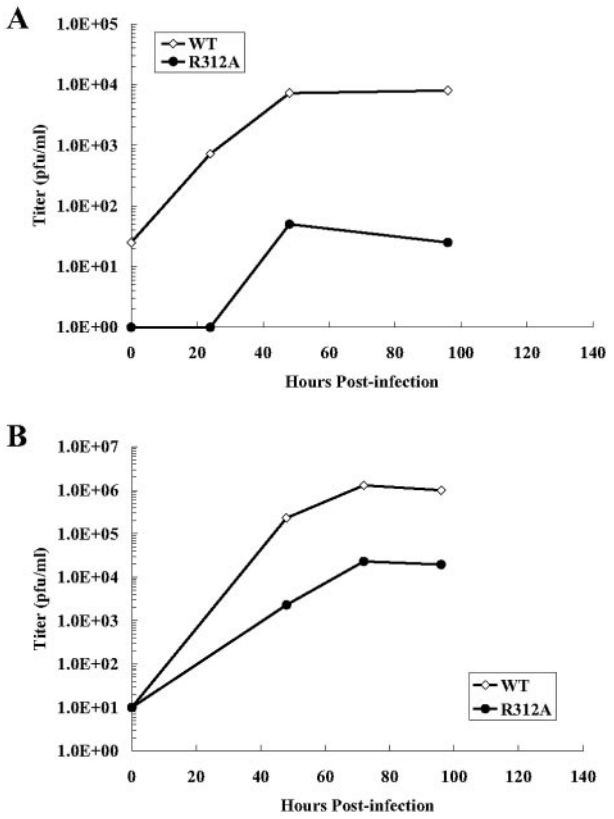

FIG. 4. Growth of recEBO-VP35/R312A virus in macrophage and hepatocyte cell lines. The growth of the recEBO-VP35/wt and recEBO-VP35/R312A viruses was measured in U937 macrophages (A) and Huh7 hepatocytes (B) infected at an MOI of 0.02.

mutant viruses at an MOI of 2. Immediately following adsorption, the cells were transfected with 300 ng of an HA-tagged IRF-3 expression plasmid. Twenty-four hours after transfection, the cells were fixed and stained using an anti-HA antibody (green) or polyclonal anti-Ebola virus (red) antibodies. The ratio of cells with nuclear to cytoplasmic IRF-3 was calculated.

In mock-infected cells and those infected with the recEBO-VP35/WT virus, approximately 5% of cells contained the active form of IRF-3 in the nucleus (Fig. 5A, rows 1 and 2, and B). However, in cells infected with either the recEBO-VP35/R305A or recEBO-VP35/R312A virus, IRF-3 was detectable in the nucleus of approximately 30% or 40% of the cells, respectively (Fig. 5A, rows 3 and 4, and B), and the cells containing nuclear IRF-3 also expressed Ebola virus antigen. Thus, as the transfection data predicted, in a live virus infection with recombinant Ebola viruses engineered to contain mutations within the IRF-3 inhibitory domain of VP35, substantially more IRF-3 is activated than that induced by infection with the recombinant virus expressing a wild-type VP35 sequence.

DISCUSSION

RNA viruses have developed numerous mechanisms to inhibit the potent innate antiviral response provided by the type I IFN system. Some viral proteins inhibit the induction of

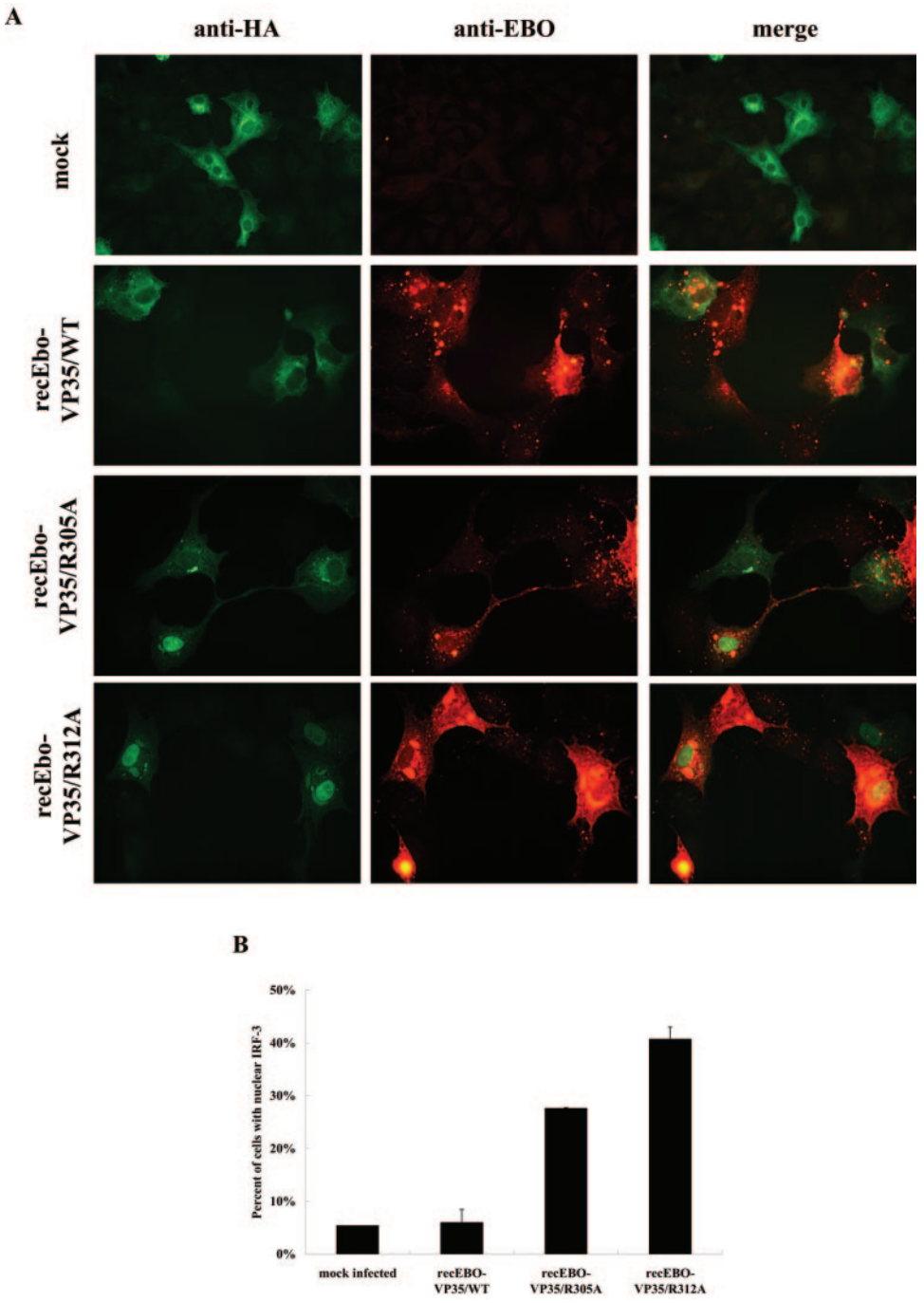

FIG. 5. Effect of infection with recombinant Ebola viruses on IRF-3 activation. A) IRF-3 localization. Vero cells were infected with the recombinant Ebola viruses at an MOI of 2 and then transfected with an HA-tagged IRF-3 plasmid. Twenty-four hours after infection, the cells on the coverslips were fixed and stained with anti-HA (green) and anti-Ebola virus (anti-EBO) (red) antibodies. Merged images are shown in the far right panels. B) Percentage of cells containing nuclear IRF-3 is shown in a graph. Approximately 100 to 200 cells were counted per coverslip to determine the ratio of nuclear versus cytoplasmic IRF-3.

IFN-β, while others inhibit signaling from its receptor. Many viruses have targeted IRF-3 because it is key to the early production of IFN-β. For example, the P protein of rabies virus prevents activation of IRF-3, and the NSP1 protein of rotavirus induces proteasomal degradation of IRF-3 (2, 13). Similarly, the VP35 protein of Ebola virus inhibits activation of IRF-3 (3).

Although VP35 is not or only weakly phosphorylated (5, 16, 34), it is analogous to the phosphoproteins (P proteins) of paramyxoviruses and rhabdoviruses (34). VP35, as well as the other P proteins, serves as an essential cofactor of the RNA-dependent RNA polymerase complex. For replication of Ebola and Marburg viruses, the polymerase L, VP35, and the nucleo-

protein NP are essential components of the replication complex. For transcription of Ebola virus, VP30 is also required in addition to L, NP, and VP35. VP35 of Marburg virus has been shown to interact with L, possibly serving as a linker between the NP and L proteins (6). In addition, VP35 of both Ebola and Marburg viruses was recently shown to form trimers via a coiled-coil motif within the amino terminus of the protein (32, 36). This trimerization was essential for transcription/replication (32) and also facilitated the IRF-3 inhibitory function of the carboxy terminus (36).

In this study, we used a minigenome-based artificial transcription/replication system to measure the ability of the mutant VP35 proteins to function as a polymerase cofactor (35). This particular minigenome system has been used extensively to study viral transcription/replication properties (31, 41, 42). This method provides an essential tool to examine the effects of mutations within VP35 on viral polymerase function without the confounding effects of IFN antagonism that would be present during a live virus infection. All of the mutations introduced into the IRF-3 inhibitory domain of VP35 resulted in proteins that were functional in viral transcription/replication in this minigenome system. It is significant to note, then, that the inhibition of IRF-3 activation mediated by the C terminus of the protein is likely distinct from the region(s) of the protein involved in transcription and replication. While it is impossible to rule out potential effects on polymerase function that are not detected by the minigenome replication, this scenario is highly unlikely given the extensive nature by which this minireplicon system has been used in the past to study detailed aspects of Ebola virus transcription and replication (7, 31, 41, 42).

Because the mutations described here did not inhibit viral transcription and replication, we were able to successfully use reverse genetics to generate recombinant Ebola viruses containing these mutations within the IRF-3 inhibitory domain of VP35. The fact that we were able to recover infectious virus using reverse genetics confirms that the VP35 proteins containing mutations do not adversely affect viral transcription/replication, otherwise no virus would have been recovered. When growth of the mutant viruses was quantitatively measured on Vero E6 cells, U937 macrophages, or Huh7 hepatocytes, significant differences were observed. With a low-MOI infection, the recEBO-VP35/R312A virus was decreased in growth by 100-fold at all time points examined compared to the recEBO-VP35/WT virus. Surprisingly, in Vero cells, the recEBO-VP35/R305A virus was also attenuated by 10-fold compared to the wild-type recEBO. The high-MOI infections showed similar patterns in virus growth, but the differences were not as dramatic as those seen with the low-MOI infections, most likely because primarily one round of infection was observed. The differences in virus growth in culture are likely due to differential activation of IRF-3 because we were able to detect higher levels of activated, nuclear IRF-3 in cells infected with the mutant viruses, whereas few were detected in cells infected with wild-type recombinant Ebola virus.

What was particularly striking was the finding that virus titer inversely correlated with the amount of RANTES protein in the supernatant. We used RANTES as a marker for IRF-3 activation, because the RANTES promoter has been shown to be directly activated by an enhanceosome consisting of IRF-3 and NF-κB (19, 29) and IRF-3 is absolutely required for virus-induced RANTES production (19). In addition, measurement of the levels of secreted RANTES protein is a physiologically relevant indicator of the production of immediate-early IRF-3-inducible proteins. It is of note that while Vero cells are fully capable of responding to IFN-β, they do not produce endogenous IFN-β due to a lack of the structural gene (33), and thus, measurement of this protein is not appropriate in this case. Vero cells are an attractive cell line for a study such as this involving IRF-3, because it eliminates the confounding effect of IFN-β production on the system and allows the examination of gene expression induced in the absence of IFN-β. At the low-MOI infection, the recEBO-VP35/R312A and recEBO-VP35/R305A viruses induced more RANTES than the wt virus by 100-fold and 10-fold, respectively. For the high-MOI infections, the differences were close to 100-fold for both mutant viruses. The fact that RANTES secretion inversely correlated with the virus titer at each time point suggests that the point mutations in VP35 are likely having an effect on the production of immediate-early IRF-3-inducible proteins.

The virus titer and RANTES ELISA results with the recEBO-VP35/R305A virus were unexpected, because the R305A protein behaved similarly to the wild-type VP35 in the ISG56-luciferase reporter gene assay (Table 1) (23). However, closer examination of the data from our previous study revealed that nearly twice as much IFN-β was secreted into the supernatants in the presence of the R305A protein than with the wild-type VP35. Thus, there was a relatively small yet detectable effect of the R305A mutation on IFN-β production that was not detected using ISG56-promoter reporter gene activation. Since the minigenome results found that the R305A protein was competent for viral replication, it is unlikely that the 10-fold decrease in virus growth seen in this study is due to defective replication of this recombinant virus, rather than a defect in IRF-3 inhibition mediated by VP35. The fact that the virus titer correlates with both IRF-3 activation and RANTES protein levels in the supernatant supports this hypothesis. However, we cannot rule out the possibility that other reasons exist for the decreased growth of this recombinant virus.

An important parallel can be drawn between the results observed here with VP35 and that of another well-studied IFN antagonist, the NS1 protein of influenza A virus. For one, VP35 can complement the growth of an influenza virus deleted for the NS1 protein (delNS1) (4). In addition, our previous study noted a similarity between the RNA-binding domain of NS1 and the C-terminal IRF-3 inhibitory domain of VP35 (23). When influenza virus NS1 is mutated at two specific residues (R38A and K41A) within the RNA-binding domain, the resulting virus is attenuated for growth in MDCK cells by 50- to 100-fold after a low-MOI infection (15). This same virus was severely attenuated when injected into susceptible mice, indicating that rather modest decreases in virus replication in cell culture can be indicative of severe attenuation in vivo (15). The effects of the VP35 mutations presented here on the pathogenesis of Ebola virus infection in mice will be evaluated; however, studies with Ebola virus are more complicated because mice are not naturally susceptible to infection. Whether the similarities between NS1 and VP35 are based on convergent evolution or are the result of a shared evolutionary history is not known, but considerable insights into the structure/function of VP35 have been gained by comparisons with NS1.

The course of infection with Ebola virus is rapid. Localized infection quickly results in high titer of viremia, and a large proportion of infected patients die before developing effective adaptive immune responses (1, 26). Because of the rapid progression of Ebola virus infection and the fact that the clinical outcome is often determined prior to development of adaptive immune responses, very early events may be important for determining the fate of EHF patients. Since macrophages and dendritic cells have been shown to be the early targets of Ebola virus infection (10, 17, 20, 38), VP35 may function to limit early IFN-β production and other antiviral signals generated from these cells, thereby slowing down the host's ability to curb virus replication and induce adaptive immunity.

In this present study, we clearly demonstrate the following. (i) The transcription/replication and IRF-3 inhibitory functions of VP35 are separable. (ii) Recombinant Ebola viruses containing mutations within the IRF-3 inhibitory domain of VP35 are attenuated for growth in several cell lines and activate IRF-3 and IRF-3-inducible gene expression at higher levels than the wild-type Ebola virus does. Future studies will delineate the importance of VP35-mediated IRF-3 inhibition in the induction of EHF.

ACKNOWLEDGMENTS

We acknowledge Chris Basler (Mt. Sinai School of Medicine) for helpful discussions regarding the manuscript. We also thank Elke Mühlberger (Philipps University Marburg) for the 3E-5E minigenome plasmid. In addition, we thank Tom Ksiazek (Special Pathogens Branch, CDC) and Pierre Rollin (Special Pathogens Branch, CDC) for support.

A.L.H. was supported in part by fellowships from the ASM/NCID postdoctoral research program and the Oak Ridge Institute of Science and Engineering (ORISE). J.E.D. was also supported by a fellowship from ORISE.

The findings and conclusions in this report are those of the authors and do not necessarily represent the views of the funding agency.

REFERENCES

1. **Baize, S., E. M. Leroy, M. C. Georges-Courbot, M. Capron, J. Lansoud-Soukate, P. Debre, S. P. Fisher-Hoch, J. B. McCormick, and A. J. Georges.** 1999. Defective humoral responses and extensive intravascular apoptosis are associated with fatal outcome in Ebola virus-infected patients. Nat. Med. **5:**423–426.
2. **Barro, M., and J. T. Patton.** 2005. Rotavirus nonstructural protein 1 subverts innate immune response by inducing degradation of IFN regulatory factor 3. Proc. Natl. Acad. Sci. USA **102:**4114–4119.
3. **Basler, C. F., A. Mikulasova, L. Martinez-Sobrido, J. Paragas, E. Muhlberger, M. Bray, H. D. Klenk, P. Palese, and A. Garcia-Sastre.** 2003. The Ebola virus VP35 protein inhibits activation of interferon regulatory factor 3. J. Virol. **77:**7945–7956.
4. **Basler, C. F., X. Wang, E. Muhlberger, V. Volchkov, J. Paragas, H. D. Klenk, A. Garcia-Sastre, and P. Palese.** 2000. The Ebola virus VP35 protein functions as a type I IFN antagonist. Proc. Natl. Acad. Sci. USA **97:**12289–12294.
5. **Becker, S., and E. Muhlberger.** 1999. Co- and posttranslational modifications and functions of Marburg virus proteins. Curr. Top. Microbiol. Immunol. **235:**23–34.
6. **Becker, S., C. Rinne, U. Hofsass, H. D. Klenk, and E. Muhlberger.** 1998. Interactions of Marburg virus nucleocapsid proteins. Virology **249:**406–417.
7. **Boehmann, Y., S. Enterlein, A. Randolf, and E. Muhlberger.** 2005. A reconstituted replication and transcription system for Ebola virus Reston and comparison with Ebola virus Zaire. Virology **332:**406–417.
8. **Bosio, C. M., M. J. Aman, C. Grogan, R. Hogan, G. Ruthel, D. Negley, M. Mohamadzadeh, S. Bavari, and A. Schmaljohn.** 2003. Ebola and Marburg viruses replicate in monocyte-derived dendritic cells without inducing the production of cytokines and full maturation. J. Infect. Dis. **188:**1630–1638.
9. **Bray, M., K. Davis, T. Geisbert, C. Schmaljohn, and J. Huggins.** 1998. A mouse model for evaluation of prophylaxis and therapy of Ebola hemorrhagic fever. J. Infect. Dis. **178:**651–661.
10. **Bray, M., and T. W. Geisbert.** 2005. Ebola virus: the role of macrophages and dendritic cells in the pathogenesis of Ebola hemorrhagic fever. Int. J. Biochem. Cell. Biol. **37:**1560–1566.
11. **Bray, M., S. Hatfill, L. Hensley, and J. W. Huggins.** 2001. Haematological, biochemical and coagulation changes in mice, guinea-pigs and monkeys infected with a mouse-adapted variant of Ebola Zaire virus. J. Comp. Pathol. **125:**243–253.
12. **Bray, M., and S. Mahanty.** 2003. Ebola hemorrhagic fever and septic shock. J. Infect. Dis. **188:**1613–1617.
13. **Brzozka, K., S. Finke, and K. K. Conzelmann.** 2005. Identification of the rabies virus alpha/beta interferon antagonist: phosphoprotein P interferes with phosphorylation of interferon regulatory factor 3. J. Virol. **79:**7673–7681.
14. **Connolly, B. M., K. E. Steele, K. J. Davis, T. W. Geisbert, W. M. Kell, N. K. Jaax, and P. B. Jahrling.** 1999. Pathogenesis of experimental Ebola virus infection in guinea pigs. J. Infect. Dis. **179**(Suppl. 1)**:**S203–S217.
15. **Donelan, N. R., C. F. Basler, and A. Garcia-Sastre.** 2003. A recombinant influenza A virus expressing an RNA-binding-defective NS1 protein induces high levels of beta interferon and is attenuated in mice. J. Virol. **77:**13257–13266.
16. **Elliott, L. H., M. P. Kiley, and J. B. McCormick.** 1985. Descriptive analysis of Ebola virus proteins. Virology **147:**169–176.
17. **Geisbert, T. W., L. E. Hensley, T. Larsen, H. A. Young, D. S. Reed, J. B. Geisbert, D. P. Scott, E. Kagan, P. B. Jahrling, and K. J. Davis.** 2003. Pathogenesis of Ebola hemorrhagic fever in cynomolgus macaques: evidence that dendritic cells are early and sustained targets of infection. Am. J. Pathol. **163:**2347–2370.
18. **Geisbert, T. W., H. A. Young, P. B. Jahrling, K. J. Davis, E. Kagan, and L. E. Hensley.** 2003. Mechanisms underlying coagulation abnormalities in Ebola hemorrhagic fever: overexpression of tissue factor in primate monocytes/macrophages is a key event. J. Infect. Dis. **188:**1618–1629.
19. **Genin, P., M. Algarte, P. Roof, R. Lin, and J. Hiscott.** 2000. Regulation of RANTES chemokine gene expression requires cooperativity between NF-kappa B and IFN-regulatory factor transcription factors. J. Immunol. **164:**5352–5361.
20. **Gibb, T. R., M. Bray, T. W. Geisbert, K. E. Steele, W. M. Kell, K. J. Davis, and N. K. Jaax.** 2001. Pathogenesis of experimental Ebola Zaire virus infection in BALB/c mice. J. Comp. Pathol. **125:**233–242.
21. **Grandvaux, N., B. R. tenOever, M. J. Servant, and J. Hiscott.** 2002. The interferon antiviral response: from viral invasion to evasion. Curr. Opin. Infect. Dis. **15:**259–267.
22. **Gupta, M., S. Mahanty, R. Ahmed, and P. E. Rollin.** 2001. Monocyte-derived human macrophages and peripheral blood mononuclear cells infected with Ebola virus secrete MIP-1alpha and TNF-alpha and inhibit poly-IC-induced IFN-alpha *in vitro*. Virology **284:**20–25.
23. **Hartman, A. L., J. S. Towner, and S. T. Nichol.** 2004. A C-terminal basic amino acid motif of Zaire Ebolavirus VP35 is essential for type I interferon antagonism and displays high identity with the RNA-binding domain of another interferon antagonist, the NS1 protein of influenza A virus. Virology **328:**177–184.
24. **Hartman, A. L., J. S. Towner, and S. T. Nichol.** 2005. Pathogenesis of Ebola and Marburg viruses, p. 109–124. *In* P. Digard, A. A. Nash, and R. E. Randall (ed.), Molecular pathogenesis of virus infections. Cambridge University Press, New York, N.Y.
25. **Khan, A. S., F. K. Tshioko, D. L. Heymann, B. Le Guenno, P. Nabeth, B. Kerstiens, Y. Fleerackers, P. H. Kilmarx, G. R. Rodier, O. Nkuku, P. E. Rollin, A. Sanchez, S. R. Zaki, R. Swanepoel, O. Tomori, S. T. Nichol, C. J. Peters, J. J. Muyembe-Tamfum, T. G. Ksiazek, and the Commission de Lutte contre les Epidemies a Kikwit.** 1999. The reemergence of Ebola hemorrhagic fever, Democratic Republic of the Congo, 1995. J. Infect. Dis. **179**(Suppl. 1)**:**S76–S86.
26. **Ksiazek, T. G., P. E. Rollin, A. J. Williams, D. S. Bressler, M. L. Martin, R. Swanepoel, F. J. Burt, P. A. Leman, A. S. Khan, A. K. Rowe, R. Mukunu, A. Sanchez, and C. J. Peters.** 1999. Clinical virology of Ebola hemorrhagic fever (EHF): virus, virus antigen, and IgG and IgM antibody findings among EHF patients in Kikwit, Democratic Republic of the Congo, 1995. J. Infect. Dis. **179**(Suppl. 1)**:**S177–S187.
27. **Ksiazek, T. G., C. P. West, P. E. Rollin, P. B. Jahrling, and C. J. Peters.** 1999. ELISA for the detection of antibodies to Ebola viruses. J. Infect. Dis. **179**(Suppl. 1)**:**S192–S198.
28. **Le Bon, A., G. Schiavoni, G. D'Agostino, I. Gresser, F. Belardelli, and D. F. Tough.** 2001. Type I interferons potently enhance humoral immunity and can promote isotype switching by stimulating dendritic cells in vivo. Immunity **14:**461–470.
29. **Lin, R., C. Heylbroeck, P. Genin, P. M. Pitha, and J. Hiscott.** 1999. Essential role of interferon regulatory factor 3 in direct activation of RANTES chemokine transcription. Mol. Cell. Biol. **19:**959–966.
30. **Mahanty, S., K. Hutchinson, S. Agarwal, M. McRae, P. E. Rollin, and B. Pulendran.** 2003. Impairment of dendritic cells and adaptive immunity by Ebola and Lassa viruses. J. Immunol. **170:**2797–2801.
31. **Modrof, J., E. Muhlberger, H. D. Klenk, and S. Becker.** 2002. Phosphorylation of VP30 impairs Ebola virus transcription. J. Biol. Chem. **277:**33099–33104.
32. **Moller, P., N. Pariente, H. D. Klenk, and S. Becker.** 2005. Homo-oligomerization of Marburg virus VP35 is essential for its function in replication and transcription. J. Virol. **79:**14876–14886.
33. **Mosca, J. D., and P. M. Pitha.** 1986. Transcriptional and posttranscriptional

regulation of exogenous human beta interferon gene in simian cells defective in interferon synthesis. Mol. Cell. Biol. **6:**2279–2283.
34. **Muhlberger, E., B. Lotfering, H. D. Klenk, and S. Becker.** 1998. Three of the four nucleocapsid proteins of Marburg virus, NP, VP35, and L, are sufficient to mediate replication and transcription of Marburg virus-specific monocistronic minigenomes. J. Virol. **72:**8756–8764.
35. **Muhlberger, E., M. Weik, V. E. Volchkov, H. D. Klenk, and S. Becker.** 1999. Comparison of the transcription and replication strategies of Marburg virus and Ebola virus by using artificial replication systems. J. Virol. **73:**2333–2342.
36. **Reid, S. P., W. B. Cardenas, and C. F. Basler.** 2005. Homo-oligomerization facilitates the interferon-antagonist activity of the Ebolavirus VP35 protein. Virology **341:**179–189.
37. Reference deleted.
38. **Ryabchikova, E. I., L. V. Kolesnikova, and S. V. Luchko.** 1999. An analysis of features of pathogenesis in two animal models of Ebola virus infection. J. Infect. Dis. **179**(Suppl. 1)**:**S199–S202.
39. **Towner, J. S., J. Paragas, J. E. Dover, M. Gupta, C. S. Goldsmith, J. W. Huggins, and S. T. Nichol.** 2005. Generation of eGFP expressing recombinant Zaire Ebolavirus for analysis of early pathogenesis events and high-throughput antiviral drug screening. Virology **332:**20–27.
40. **Towner, J. S., P. E. Rollin, D. G. Bausch, A. Sanchez, S. M. Crary, M. Vincent, W. F. Lee, C. F. Spiropoulou, T. G. Ksiazek, M. Lukwiya, F. Kaducu, R. Downing, and S. T. Nichol.** 2004. Rapid diagnosis of Ebola hemorrhagic fever by reverse transcription-PCR in an outbreak setting and assessment of patient viral load as a predictor of outcome. J. Virol. **78:**4330–4341.
41. **Watanabe, S., T. Watanabe, T. Noda, A. Takada, H. Feldmann, L. D. Jasenosky, and Y. Kawaoka.** 2004. Production of novel Ebola virus-like particles from cDNAs: an alternative to Ebola virus generation by reverse genetics. J. Virol. **78:**999–1005.
42. **Weik, M., S. Enterlein, K. Schlenz, and E. Muhlberger.** 2005. The Ebola virus genomic replication promoter is bipartite and follows the rule of six. J. Virol. **79:**10660–10671.
43. **Zaki, S. R., and C. S. Goldsmith.** 1999. Pathologic features of filovirus infections in humans. Curr. Top. Microbiol. Immunol. **235:**97–116.